Does carbon dioxide storage by cyanobacteria induce biomineralization in presence of basaltic glass?

Thomas Ferrini, Olivier Grandjouan, Olivier Pourret, Raul E Martinez

Does carbon dioxide storage by cyanobacteria induce biomineralization in presence of basaltic glass?

Thomas Ferrini[1], Olivier Grandjouan[1], Olivier Pourret[1,#], Raul E. Martinez[2,*]

[1]UniLaSalle, AGHYLE, 19 rue Pierre Waguet, 60026 Beauvais cedex, France

[2]Institut für Geowissenschaten, Universität Freiburg, Alberstraße 23b, 79104 Freiburg, Germany

*Present address: Max Planck Institute for Biogeochemistry

#Corresponding author: olivier.pourret@unilasalle.fr.

Abstract

Cyanobacteria induced biomineralization of atmospheric CO_2 is a natural process leading to the formation of carbonates by spontaneous precipitation or through the presence of nucleation sites, under supersaturated conditions. As importance of basaltic rocks in the carbon cycle has already been highlighted, basaltic glass was chosen to test its ability to release cations needed for carbonate formation in presence of *Synechococcus* sp. cyanobacteria. Active cyanobacteria were expected to generate a local alkaline environment through photosynthetic metabolism. This process produces oxygen and hydroxide ions as waste products, raising the pH of the immediate cell surface vicinity and indirectly enhancing the carbonate CO_3^{2-} concentration and providing the a degree of saturation that can lead to the formation of calcite $CaCO_3$ or magnesite $MgCO_3$. In the presence of active cells, the saturation index (SI) increased from -10.56 to -9.48 for calcite and from -13.6 to -12.5 for magnesite, however they remained negative due to the low Ca^{2+} and Mg^{2+} activities. Dead cells were expected to act as nucleation sites by the stepwise binding of carbonate with Ca^{2+} and Mg^{2+} on their surface. In the presence of inactive cells, SI values were closer to 0 but still negative due to the low pH and cation concentrations. Our results highlight that our current understanding of the carbon cycle suggests that Earth's climate is stabilized by a negative feedback involving CO_2 consumption and especially during chemical weathering of silicate minerals.

Keywords: biomineralization, cyanobacteria, basaltic glass, carbonate, saturation index, critical zone

1. Introduction

The rise of CO_2 concentrations in the atmosphere is one of the most important environmental problems on Earth today arising from anthropic activity (Gerlach, 2011). Carbon storage methods, or carbon concentration mechanisms (CCM), need to be developed urgently in order to reduce the CO_2 impact on Earth's terrestrial and aquatic environments. The ability of cyanobacteria to induce the biomineralization of CO_2 is an option which is still in its infancy and could possibly be used in the near-future to decrease atmospheric CO_2 levels (Martinez *et al.*, 2016). Previous studies have proven the link between cyanobacteria photosynthesis and the presence of metallic cations could lead to carbonate precipitation in the presence of atmospheric CO_2 and under suitable solution conditions (Jansson and Northen, 2010; Martinez *et al.*, 2016; Obst *et al.*, 2009).

Photosynthesis and CCM are the first steps to biomineralization of CO_2. Cyanobacteria are autophototrophic microorganisms. They are primary producers, which generate their own nutrients by carrying out the oxygenic photosynthesis (Martinez *et al.*, 2016). This metabolism needs carbon as a source of inorganic carbon in the form of dissolved CO_2, natural light as source of energy and water to provide electrons needed in the redox transformation of carbon (Schubert *et al.*, 1997). The Calvin-Benson cycle permits the assimilation of the inorganic carbon thanks to the initial CO_2-fixing-enzyme of photosynthesis: RuBisCO (Ribulose Biphosphate Carbolxylase Oxygenase) (Fridlyand and Scheibe, 1999; Spreitzer and Salvucci, 2002). Chemical and photochemical reactions take place in photosystems located on the thylakoid membrane of the cyanobacteria cell. ATP (Adenosine triphosphate) and NADPH (Nicotinamide adenine dinucleotide phosphate) are chemical substances which permit CO_2 assimilation. A constant supply of inorganic carbon (IC) is required to carry out photosynthesis.

Dissolved CO_2, in the form of bicarbonate HCO_3^- is the inorganic form of carbon used by cyanobacteria as an IC source. A metabolic system is used to attain inorganic carbon from the aqueous environment. The CCM corresponds to an environmental adaptation of cyanobacteria, it allows IC incorporation inside the cell in the form of HCO_3^- and convert it to CO_2 (Price *et al.*, 2008). Molecules are attracted and stocked inside the cell with the help of IC transporters located in both plasma and outer membranes. HCO_3^- transport is enhanced by the extra-ATP generated during photosynthesis. The inorganic carbon is transported into the bacterial micro-compartment where the bicarbonate molecules are transformed into CO_2 by the enzyme carbonic anhydrase. The remaining CO_2 is then assimilated by the enzyme RuBisCO for photosynthesis (Figure 1). A proton H^+ is consumed by each of these reactions, leading to the release of a hydroxide ion (OH^-) outside the cell as a waste product along with O_2. This allows the generation of an alkaline pH within the micro-environment around the cyanobacteria cell. This alkaline pH permits the deprotonation of the external bicarbonate HCO_3^- to carbonate ions CO_3^2. The presence of both metal cations (e.g. Ca^{2+}/Mg^{2+}) and carbonate (CO_3^{2-}) allows the nucleation of carbonates in the form of calcite ($CaCO_3$) and magnesite ($MgCO_3$) (Martinez *et al.*, 2016; Riding, 2006). However, the amount of metal cations and carbonate must be high enough to reach supersaturation with respect to these carbonate minerals.

In this study, basaltic glass was chosen as a source of metallic cations due to its composition and abundance on the Earth's surface. Its importance in the carbon cycle has been proven on several previous studies (Dessert *et al.*, 2003; Grimm *et al.*, 2019; Schlesinger and Bernhardt, 2013; Schott *et al.*, 2012). A high rate of dissolution of basaltic glass would be required to release significant metallic cation concentrations to achieve supersaturation with respect to carbonate phases. Varying an electrolyte $NaNO_3$ background concentration has been shown to affect the process of simple silicate mineral dissolution and the rate of release of metallic cations as well as their activity (Martinez *et al.*, 2014; Martinez *et al.*, 2016). An

optimal concentration is needed in order to reach Ca^{2+} and Mg^{2+} activities, which together with carbonate ion activities would lead to precipitation of carbonates. The *Synechococcus* cyanobacteria species chosen for this study is representative of seawater cyanobacteria as along with *Prochloroccocculs* sp., it is responsible for approximately 30% of the photosynthesis on Earth. *Synechococcus* sp. is a unicellular coccoid cyanobacteria containing outermost surface layers but no cell covering sheath (Martinez *et al.*, 2010; Martinez *et al.*, 2008). The goal of this study is to determine whether basaltic glass is an efficient source of metal cations needed for CO_2 mineralization and then to quantify the rates of carbonate precipitation in presence of this primary silicate and *Synechococcus* cyanobacteria species so that optimal conditions in terms of basaltic glass dissolution and cyanobacteria biomass can be found.

2. Material and methods

A 20 mL aliquot of active *Synechococcus* sp. cyanobacteria stock at the stationary phase was placed in a 5 L Schott® bottle. *Synechococcus* sp. cultures were grown in Cyanobacteria BG-11 Freshwater Medium (Sigma-Aldrich C3061) for three weeks to stationary growth phase (Martinez *et al.*, 2010). Active cyanobacteria stocks were prepared in order to achieve photosynthesis in presence of basaltic glass (see bulk composition in Table 1), in order to quantify the influence of cyanobacteria on the dissolution of the mineral could be observed and the supersaturation conditions reached (see discussion on choice of experimental conditions in Martinez *et al.*, 2010). Stock cultures of cyanobacteria were kept at room temperature (23±1°C) under constant cool white fluorescent light illumination (5000 lx) and a constant filtered air injection (3 L/min at around 400 ppm) in order to provide cyanobacteria with needed inorganic carbon. The air inflow was used to keep the culture in a constant movement needed for optimal growth. For each experiment, 5 L of 1/500 diluted cyanobacteria growth medium inoculated

with a 20 mL aliquot of regular 1/50 BG-11 (Table 2) cyanobacteria stock was placed on a rotary shaker at 250 rpm (Martinez *et al.*, 2008). Dead cyanobacteria were prepared by autoclaving an aliquot of active stock at 121°C for 20 min. To measure the exact cyanobacteria mass, a 25 mL sample was collected. Vacuum filtration was used to filter the sample through a 0.2 µm pore size cellulose nitrate filter (Whatman®). The filtered sample was placed in an oven at 60°C for 30 min and then weighed.

2.1. Flow through open reactors system experimental design

Basaltic glass dissolution experiments were performed at 23±1°C by mixing two different stock solutions in flow through reactors with a peristaltic pump with a fixed inflow rate of 1.4 µL/min. The active cyanobacteria and inorganic stocks solutions used are described in **Tables 2 and 3**.

To quantify the rates of basaltic glass and carbonate precipitation in presence of *Synechococcus sp*. cyanobacteria, duplicate flow through reactors were used, each connected to the inorganic and active cyanobacteria stocks by a peristaltic pump (Active cyanobacteria Flow Through open reactor, AFT; **Table 2 and Figure 2**).

To assess the role of bio-mineralization by dead cells, a calcium chloride stock solution was used instead of basaltic glass as the source of metal cations (e.g. Ca^{2+}). For these experiments, a flow through reactor was connected through the peristaltic pump to both the calcium chloride and dead cyanobacteria stocks previously washed by centrifuging at 10,000 rpm for 20 min (Calcium Flow Through reactor, CFT; **Table 3 and Figure 3**). Preliminary results and tests are available in Ferrini and Grandjouan (2015). These dead cells act as nucleation sites. They

decrease the activation energy for precipitation, but saturation index (SI) values are not influenced by the existence of nucleation sites (Martinez *et al.*, 2008).

For all experiments, Tygon R 3603 tubes were used to link both stocks to 200 mL flow through reactors with the help of a 4 channel peristaltic pump with a low flow rate of 1.4 µL/min.

2.2. Sample analysis

In order to monitor the chemical evolution and the cyanobacteria biomass concentration of the solution inside the flow through reactor, the pH, conductivity, alkalinity, optical density, and Ca^{2+} and Mg^{2+} concentrations were measured from samples collected in 50 mL polypropylene Falcon® tubes from the output of the flow through reactors, once daily. Time zero was taken to be the time of this first sampling of the flow through reactor solution (Martinez *et al.*, 2016). Reactors were placed in a water bath at 22°C in order to keep their contents solutions at a constant temperature. A 20 mL sample was taken from each reactor for all experiments. An aliquot of 7 mL of sample was used to measure the optical density of the solution at 750 nm wavelength, to approximate the concentration of cyanobacteria biomass over time. The remaining 13 mL were used to measure pH, total alkalinity and conductivity. The pH and alkalinity were measured with an automatic titration system (Metrohm® 719 Titrino automatic titrator). In this study, dominated by the presence of dissolved CO_2, the total alkalinity (TA) provides an estimate of the concentrations of bicarbonate and carbonate species in solution. The TA is determined through an acid titration (alkalinity titration) where the final concentration of the acid, at the second end-point of the carbonate system, pH = 4.3, represents the total alkalinity of the solution. Carbonate alkalinity (CA) is determined by driving the alkalinity titration to the

first end-point for the carbonate system at pH = 8.3. From the carbonate alkalinity, the CO_3^{2-} concentration in solution, which is part of total alkalinity, can be determined:

$$TA = [HCO_3^-] + 2\,[CO_3^{2-}] + [OH^-] - [H^+] \quad (1a)$$

$$CA = 2\,[CO_3^{2-}] + [OH^-] \quad (1b)$$

As $[CO_3^{2-}]$, $[H^+]$ and $[OH^-]$ are negligible for neutral to alkaline pH conditions (between 6 and 11), total alkalinity can be re-defined to:

$$TA = [HCO_3^-] \quad (2)$$

Ca^{2+} and Mg^{2+} concentrations were measured by flame atomic adsorption spectroscopy (F-AAS) with an Analytik Jena Vario 6 flame atomic adsorption spectrometer. The conductivity of sample aliquots was measured using a WTW LF 325 conductivity meter where conductivity is measured in mS/cm (Harris, 2010). Conductivity measurements for a particular solution allow calculation of the ionic strength (IS). The IS is proportional to the concentration of all dissolved salts in a solution. The ionic strength is required to calculate cation activity (ac) as shown below:

$$a_C = [C]\cdot\gamma_C \quad (3)$$

where [C] is the species concentration and γ_C is the activity coefficient. The $\log_{10}$ of γ_C can be calculated as per the Debye-Hückel equation Eq. 4 as a function of the solution IS determined from conductivity measurements:

$$\log \gamma_C = (-0.51 * z^2 * \sqrt{IS})/(1+(\alpha * \sqrt{IS}/305)) \quad (4)$$

where z represents the charge of the ion (e.g. for Mg^{2+}, z=2), α the radius of the ion in picometers (e.g. for Ca^{2+}, α_{Ca2+} = 600 pm) (Harris, 2010; Stumm and Morgan, 1996).

To predict the formation of carbonate phases in this study, it is first necessary to quantify the degree of solution supersaturation with respect to Ca or Mg carbonates. This requires knowledge of the saturation index for each of these mineral phases. However, calculation of saturation state is first necessary. The saturation state (Ω) represents the degree of saturation of a solution with respect to a particular mineral phase (Langdon *et al.*, 2000) and is defined as follows:

$$\Omega = (aCa^{2+} * aCO_3^{2-})/Ksp \qquad (5)$$

Where Ksp is the solubility product of the mineral phase that can potentially form in solution (e.g. for calcite, $Ksp=10^{-8.48}$) and, aCa^{2+} and aCO_3^{2-} are the activities of Ca^{2+} and CO_3^{2-} respectively. The SI is then defined as:

$$SI = log_{10}(\Omega) \qquad (6)$$

A positive value of SI indicates supersaturation with respect to a mineral phase and suggests that precipitation of the mineral would occur. However this depends further on solution conditions (e.g. mineral nucleation, spontaneous nucleation/precipitation) (Langdon *et al.*, 2000).

3. Results

Temporal evolution of the pH, the total alkalinity and the cations concentrations has been measured. These values were used to calculate saturation index with respect to calcite and magnesite. Related values for AFT and CFT are presented in Figures 4 and 5 and Figures 6 and 7, respectively. For all conditions, experiments were carried out in duplicates.

3.1. Active cyanobacteria Flow Through open reactor results

In this experiments, the pH remained alkaline, starting at 10.9 ±1 and declining until a pH of 10.1 at 150 h (Figure 4). Total alkalinity increased from 1 mmol/L to 1.8 mmol/L in 242 h for both reactors (Figure 4). [Ca^{2+}] and [Mg^{2+}] remained constant for the duration of the experiments at an average of 3.37 +/- 1.00 mg/L for [Ca^{2+}] and 3.28 +/- 0.44 mg/L for [Mg^{2}]. A slight decrease in these concentrations was observed for the experiment in the first reactor. SI values for both calcite and magnesite remained negative for the time of the experiment. The $SI_{(calcite)}$ increased from -10.6 to -9.4 over a period of 145 h whereas the $SI_{(magnesite)}$ raised from -13.6 to -12.5 (Figure 5). Both SI curves reached a constant threshold at 150 h.

3.2. Calcium Flow Through reactor results

The pH and the total alkalinity increased through the 300 h of the experiments. A total alkalinity of 0.2 mmol/L was recorded at the start of experiments to reach a final value of 0.75 mmol/L (Figure 6). The pH was for the most part neutral but raised from 6.3 to a last value of 6.75

228 (Figure 6). The calcium chloride used permitted to obtain a rather constant [Ca^{2+}] concentration
229 at an average of 280 mg/L. The calculated $SI_{(calcite)}$ is negative but close to the solution
230 supersaturation with respect to calcite. These values are remained within the range of -4.6 to -
231 4.9 for the duration of the experiment (Figure 7).

232

4. Discussion

None of both experiments could achieve supersaturation state with respect to calcite or magnesite. The SI remain negative but fluctuate as a function of the pH, the cation concentration and the total alkalinity. This confirms that saturation index depends on metal cations and CO_3^{2-} activities and further suggests the inability of basaltic glass dissolution to provide the necessary amount of cations required for solution supersaturation with respect to carbonates. The AFT experiment shows constant [Ca^{2+}] and [Mg^{2}] concentrations (see details in Ferrini and Grandjouan (2015)). In this case an increase in the CO_3^{2-} activity would be required to achieve supersaturated conditions with respect to carbonate, this would be reflected in a positive value of the SI for these mineral phases. As the concentration of cations remained constant, a higher concentration of carbonate or a higher degree of bicarbonate deprotonation from a higher pH would be required. This means an enhanced deprotonation of bicarbonate HCO_3^- and the consumption of hydroxide ion (OH^-). This then explains the decreasing pH and the increasing total alkalinity as per eq.1. According to the previously mentioned definition of the carbonate alkalinity a pH higher than 8.3 would be required in order to induce bicarbonate ion deprotonation for production of CO_3^{2-} in significant concentrations (Stumm and Morgan, 1996). A higher pH could be reached by active cyanobacteria. Indeed, cyanobacteria consume bicarbonate ions by photosynthesis which leads to the higher pH values, the formation of carbonate (CO_3^{2-}) and a raising SI in the presence of sufficient metal cations for supersaturation In the CFT case, increasing pH rates can be explained by the presence of dead cyanobacteria mass and their interaction of their deprotonated cell surface groups with dissolving CO_2 from air injection (Weber and Martinez, 2017). However, SI remains negative because of the near-neutral pH which prevents calcite precipitation as bio-mineralization needs a pH higher than 8.3 to commence the generation of carbonate ions.

It has been shown that active cyanobacteria have a protective mechanism against carbonate precipitation on their surface, which is missing for dead cyanobacteria implying that this is the consequence of the metabolic activity of these primary producers (Martinez *et al.*, 2010; Martinez *et al.*, 2008). Dead cyanobacteria cells or cellular debris may act as nucleation sites by binding Ca^{2+} and Mg^{2+} cations on their surface. This could explain why the SI results become less negative in the CFT experiment in presence of dead cells. There are two mechanisms of mineral precipitation which are favored depending on the degree of solution supersaturation with respect to a particular mineral. In our study, we did not observe supersaturation with respect to carbonate minerals, nor the conditions for spontaneous nucleation of these minerals, a process that takes place saturation state values equal or in excess of 3 to 4. However, the existence of nucleation sites, does decrease the activation energy for precipitation, therefore affecting the saturation index for a particular mineral, not in the bulk solution, but in the microenvironment of dead cell surfaces, for example, where the value of the SI for a specific carbonate mineral may be enhanced due to the higher concentration of metal cations and carbonate, near the negatively charged reactive solid surface. Therefore, the presence of both active and dead cyanobacteria, as in the natural environment, contributes to controlling the mode of carbonate mineral precipitation, through the generation of an alkaline pH or due to the efficient sorption of metal cations leading to the nucleation of mineral phases (Martinez *et al.*, 2010; Martinez *et al.*, 2016; Weber and Martinez, 2017).

Another important factor which is needed for supersaturation is the metal cations concentrations. CFT results proved that high metal cation concentrations from an efficiently dissolving source, such as calcium chloride, lead to SI values which are closer to solution supersaturation with respect to carbonates. AFT [Ca^{2+}] and [Mg^{2+}] concentrations from basaltic glass dissolution were insufficient to achieve carbonate precipitation. Indeed, a solution needs to be supersaturated with respect to a particular mineral in order for it to precipitate. Therefore,

283 the precipitation of carbonate minerals will depend not only on the metal cation activity but
284 also on the carbonate activity. In our results the pH of the solutions was low, therefore we
285 observed a low carbonate activity and a slight release of metal cations from the basaltic glass.
286 Therefore, both of these aspects did not allow the ion activity product of metal cation and
287 carbonate in solution, to exceed the solubility product for carbonate minerals. This implies that
288 the use of basaltic glass for carbonation and CO_2 mineralization would be inefficient if
289 employed at large scale, requiring the use of faster dissolving simple silicate minerals such as
290 olivine, or finding a way to enhance the release of metal cations from simple and more
291 complicated alumino-silicate minerals. The slight decrease in metal cation concentrations in
292 these experiments, occasionally observed, can be explained by the need for more testing and
293 development of the flow through reactor used, where a fast flow rate would cause dilution of
294 metal cations. A slower pump rate would have to be used. Moreover, higher metal cation
295 dissolution rates would have to be reached, however, another silicate mineral would need to be
296 tested which can release metal cations at a faster rate. The background electrolyte concentration
297 of 0.04 mol/L $NaNO_3$ could be modified in order to find the optimal concentration and optimize
298 the dissolution rate and the metal cation activities. Smaller basaltic glass particles can be used,
299 this would produce and increase mineral surface area which would lead to an increase in the
300 basaltic glass dissolution rate.

301 As proposed on Figure 1, parameters which could contribute to achieving supersaturation state
302 with respect to carbonates and subsequent precipitation in the presence of cyanobacteria are
303 highlighted. As evidenced by our study, several points have to be improved in order to achieve
304 carbonate nucleation and precipitation. *Synechococcus* cyanobacteria have to be grown in
305 proper conditions with enough space and time to get to cell population saturation (at least 2
306 weeks). Active cells lead to an alkaline (high pH) environment by the photosynthesis process,
307 and indirectly to the formation of carbonate CO_3^{2-}. The "flow through reactor" open system

permits a constant CO_2 supply and other nutrients required for photosynthesis and cell growth. On another hand, basaltic glass has to be dissolved in optimal conditions so as to reach high aqueous [Ca^{2+}] and [Mg^{2+}] concentrations. Providing all these conditions, calcite or magnesite precipitation could be expected in the flow through reactors. Using the rate model in Eq.11 an approximation of the total carbonate precipitation amount could be calculated for potential implementation of these systems at the larger scale. Scanning electron microscopy and energy-dispersive X-ray spectroscopy analyses could then help to the analysis and identification of carbonates to confirm the presence of calcite or aragonite polymorphs or that of magnesite. By finding optimal conditions for cyanobacteria induced bio-mineralization, this method could be used to stock significant quantities of CO_2 at a large scale.

Overall, our results highlight that our current understanding of the long-term carbon cycle suggests that Earth's climate is stabilized by a negative feedback involving CO_2 consumption and especially during chemical weathering of silicate minerals (Penman *et al.*, 2020).

Acknowledgments

The authors would like to thank the Institut Polytechnique UniLaSalle, for funding part of this study and T.F. and O.G. bachelor thesis. In addition the authors would like to thank Ms. Sigrid Hirth-Walther of the Institute of Geosciences at the University of Freiburg for F-AAS measurements, Dr. Petru Jitaru of Institut Polytechnique UniLaSalle for ICP-MS analysis. Furthermore, the authors would like to extend their gratitude to Dr. Christian Grimm and Dr. Eric H. Oelkers of the GET-CNRS in Toulouse, France, for providing the basaltic glass samples used in this study. Eventually, we thank Dr. Daniel E. Ibarra for insightful review of the manuscript.

References

Dessert, C., Dupré, B., Gaillardet, J., François, L. M. and Allègre, C. J. (2003) Basalt weathering laws and the impact of basalt weathering on the global carbon cycle. *Chem. Geol.* **202**, 257-273.

Ferrini, T. and Grandjouan, O. (2015) CO_2 storage by cyanobacteria induced biomineralization in presence of basaltic glass. Bachelor.

Fridlyand, L. E. and Scheibe, R. (1999) Regulation of the Calvin cycle for CO2 fixation as an example for general control mechanisms in metabolic cycles. *Biosystems*. **51**, 79-93.

Gerlach, T. (2011) Volcanic versus anthropogenic carbon dioxide. *Eos, Transactions American Geophysical Union*. **92**, 201-202.

Grimm, C., Martinez, R. E., Pokrovsky, O. S., Benning, L. G. and Oelkers, E. H. (2019) Enhancement of cyanobacterial growth by riverine particulate material. *Chem. Geol.* **525**, 143-167.

Harris, D. C. (2010) *Quantitative Chemical Analysis, Eight Edition*. MacMillan Publishing

Jansson, C. and Northen, T. (2010) Calcifying cyanobacteria—the potential of biomineralization for carbon capture and storage. *Current Opinion in Biotechnology*. **21**, 365-371.

Langdon, C., Takahashi, T., Sweeney, C., Chipman, D., Goddard, J., Marubini, F., Aceves, H., Barnett, H. and Atkinson, M. J. (2000) Effect of calcium carbonate saturation state on the calcification rate of an experimental coral reef. *Global Biogeochem. Cy.* **14**, 639-654.

Martinez, R. E., Gardés, E., Pokrovsky, O. S., Schott, J. and Oelkers, E. H. (2010) Do photosynthetic bacteria have a protective mechanism against carbonate precipitation at their surfaces? *Geochim. Cosmochim. Acta*. **74**, 1329-1337.

Martinez, R. E., Pokrovsky, O. S., Schott, J. and Oelkers, E. H. (2008) Surface charge and zeta-potential of metabolically active and dead cyanobacteria. *J. Colloid Interface Sci.* **323**, 317-325.

Martinez, R. E., Weber, S. and Bucher, K. (2014) Quantifying the kinetics of olivine dissolution in partially closed and closed batch reactor systems. *Chem. Geol.* **367**, 1-12.

Martinez, R. E., Weber, S. and Grimm, C. (2016) Effects of freshwater Synechococcus sp. cyanobacteria pH buffering on CaCO3 precipitation: Implications for CO2 sequestration. *Appl. Geochem.* **75**, 76-89.

Obst, M., Wehrli, B. and Dittrich, M. (2009) CaCO3 nucleation by cyanobacteria: laboratory evidence for a passive, surface-induced mechanism. *Geobiology*. **7**, 324-347.

Penman, D. E., Caves Rugenstein, J. K., Ibarra, D. E. and Winnick, M. J. (2020) Silicate weathering as a feedback and forcing in Earth's climate and carbon cycle. *Earth-Science Reviews*. **209**, 103298.

Price, G. D., Badger, M. R., Woodger, F. J. and Long, B. M. (2008) Advances in understanding the cyanobacterial CO2-concentrating-mechanism (CCM): functional components, Ci transporters, diversity, genetic regulation and prospects for engineering into plants. *Journal of Experimental Botany*. **59**, 1441-1461.

Riding, R. (2006) Cyanobacterial calcification, carbon dioxide concentrating mechanisms, and Proterozoic–Cambrian changes in atmospheric composition. *Geobiology*. **4**, 299-316.

Schlesinger, W. H. and Bernhardt, E. S. (2013) Chapter 5 - The Biosphere: The Carbon Cycle of Terrestrial Ecosystems. *Biogeochemistry (Third Edition)* (Schlesinger, W. H. and Bernhardt, E. S. eds.), 135-172, Academic Press.

Schott, J., Pokrovsky, O. S., Spalla, O., Devreux, F., Gloter, A. and Mielczarski, J. A. (2012) Formation, growth and transformation of leached layers during silicate minerals dissolution: The example of wollastonite. *Geochim. Cosmochim. Acta*. **98**, 259-281.

Schubert, W.-D., Klukas, O., Krauß, N., Saenger, W., Fromme, P. and Witt, H. T. (1997) Photosystem I of Synechococcus elongatus at 4 Å resolution: comprehensive structure analysis. *Journal of Molecular Biology*. **272**, 741-769.

Spreitzer, R. J. and Salvucci, M. E. (2002) RUBISCO: Structure, Regulatory Interactions, and Possibilities for a Better Enzyme. *Annual Review of Plant Biology*. **53**, 449-475.

Stumm, W. and Morgan, J. J. (1996) *Aquatic Chemistry*. Wiley Intersciences

Weber, S. and Martinez, R. E. (2017) Effects of Synechococcus sp. cyanobacteria inert biomass on olivine dissolution: Implications for the application of enhanced weathering methods. *Appl. Geochem.* **84**, 162-172.

385

386

387 **Table 1** Bulk composition of basaltic glass

Element	Unit	Concentration
SiO_2	%	47.49
Al_2O_3	%	14.06
Fe_2O_3	%	13.51
MgO	%	9.38
CaO	%	11.62
Na_2O	%	1.85
K_2O	%	0.28
TiO_2	%	1.53
P_2O_5	%	0.17
MnO	%	0.2
Cr_2O_3	%	0.086

388

389

390

391

392 **Table 2** Composition of flow through reactors initial solution for AFT experiment.

5L of active cyanobacteria stock	
Reagent	Quantity
aliquot BG-11	10 mL
Synechococcus sp. at the stationary phase	20 mL
$NaNO_3$	0.04 mol/L
$MgSO_4$	0.003 mol/L
"Inorganic" stock	
Basaltic glass	20 g
$NaNO_3$	0.04 mol/L
$MgSO_4$	0.003 mol/L

393

394

395 **Table 3** Composition of flow through reactors initial solution for CFT experiment.

5 L dead cyanobacteria "autoclaved" stock	
Reagent	Quantity
Active cyanobacteria "autoclaved" (20 min at 121°C)	60 mL
$NaNO_3$	0.04 mol/L
$MgSO_4$	0.003 mol/L
Calcium chloride stock	
CaCl	0.09 mol/L
NaNO3	0.04 mol/L
MgSO4	0.003 mol/L

Figure captions

Figure 1 Schematic interpretation of optimal conditions leading to cyanobacteria induced bio-mineralization in presence of basaltic glass.

Figure 2 Active cyanobacteria Flow Through open reactor (AFT) experimental set up.

Figure 3 Calcium Flow Through reactor (CFT) experimental set up.

Figure 4 Evolution of pH and total alkalinity through time experiment (0.04 mol/L $NaNO_3$; AFT experiment 2). Experiment was duplicated between 0 and 120 h.

Figure 5 Evolution of saturation index through time experiment (0.04 mol/L $NaNO_3$; AFT experiment 2).

Figure 6 Evolution of pH and total alkalinity through time experiment (0.04 mol/L $NaNO_3$; CFT experiment).

Figure 7 Evolution of Saturation index through time experiment (0.04 mol/L $NaNO_3$; CFT experiment).

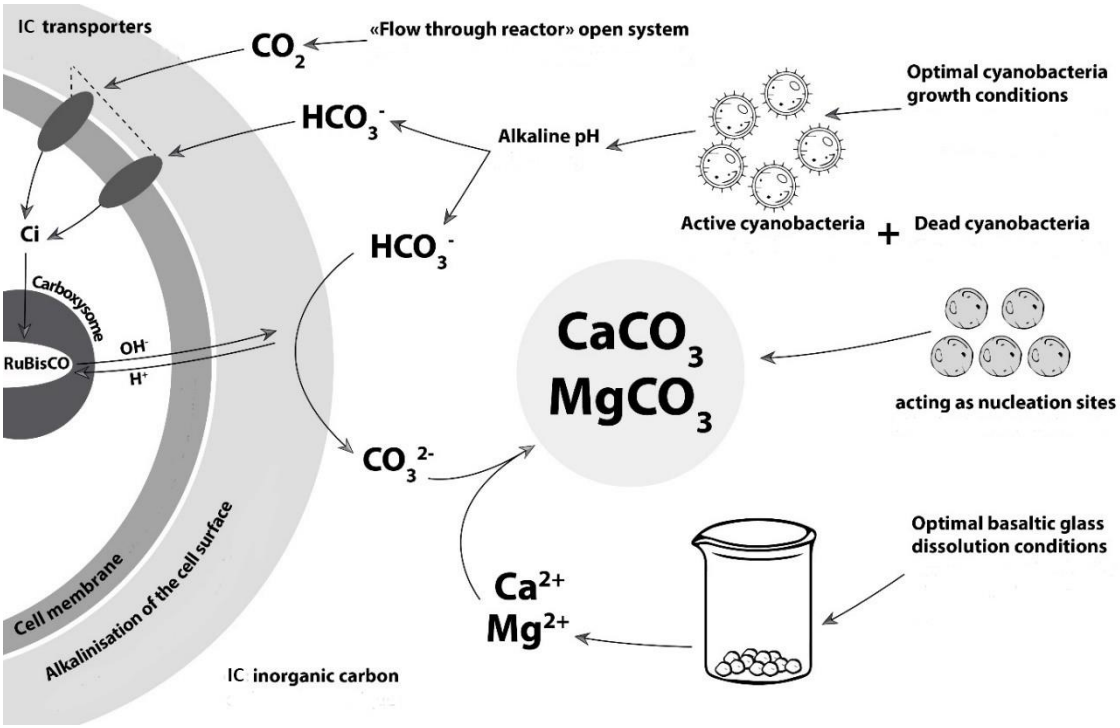
IC transporters
CO_2
«Flow through reactor» open system
HCO_3^-
Alkaline pH
Optimal cyanobacteria growth conditions
Active cyanobacteria + Dead cyanobacteria
Ci
HCO_3^-
Carboxysome
RuBisCO
OH^-
H^+
$CaCO_3$
$MgCO_3$
acting as nucleation sites
CO_3^{2-}
Optimal basaltic glass dissolution conditions
Ca^{2+}
Mg^{2+}
Cell membrane
Alkalinisation of the cell surface
IC inorganic carbon

Figure 1

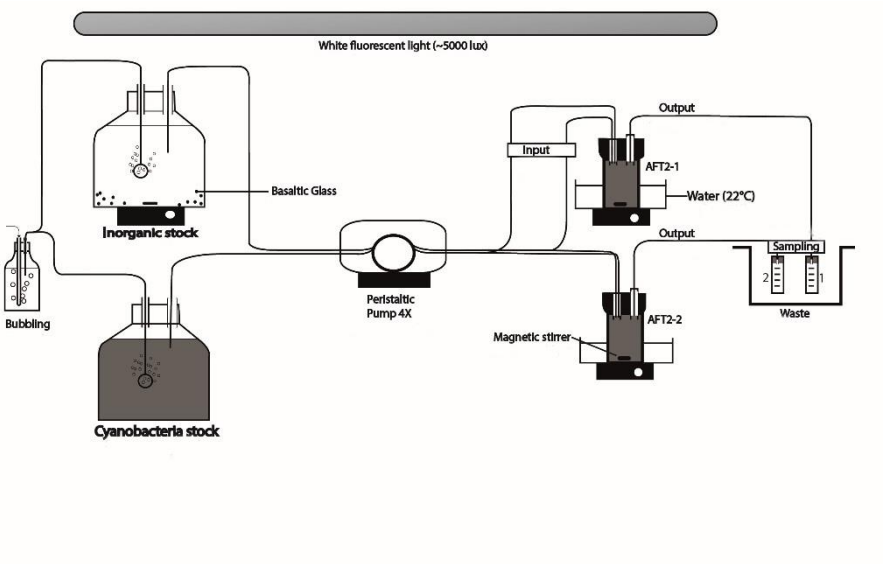
White fluorescent light (~5000 lux)
Output
Input
AFT2-1
Water (22°C)
Basaltic Glass
Inorganic stock
Output
Sampling
2
1
Waste
Bubbling
Peristaltic
Pump 4X
AFT2-2
Magnetic stirrer
Cyanobacteria stock

Figure 2

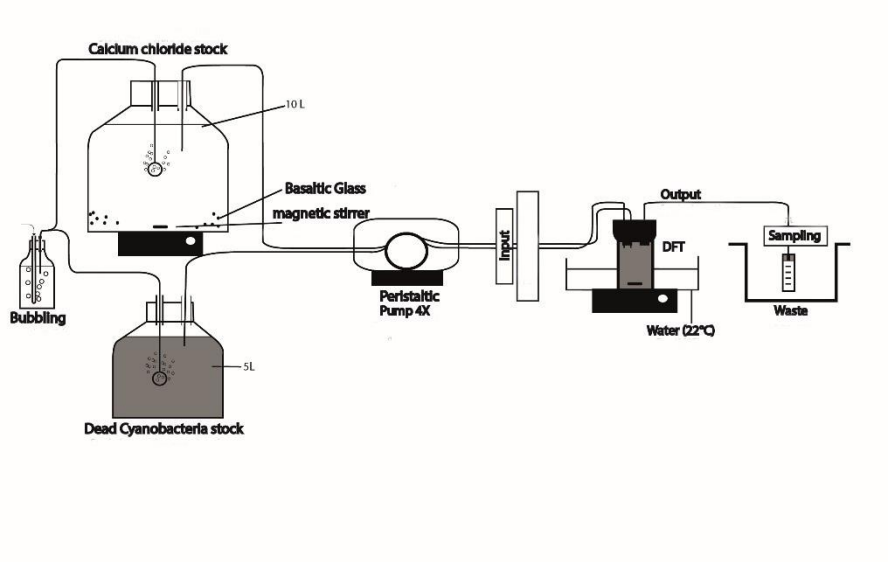
Calcium chloride stock
10 L
Basaltic Glass
magnetic stirrer
Bubbling
Peristaltic
Pump 4X
Input
Output
DFT
Water (22°C)
Sampling
Waste
5L
Dead Cyanobacteria stock

Figure 3

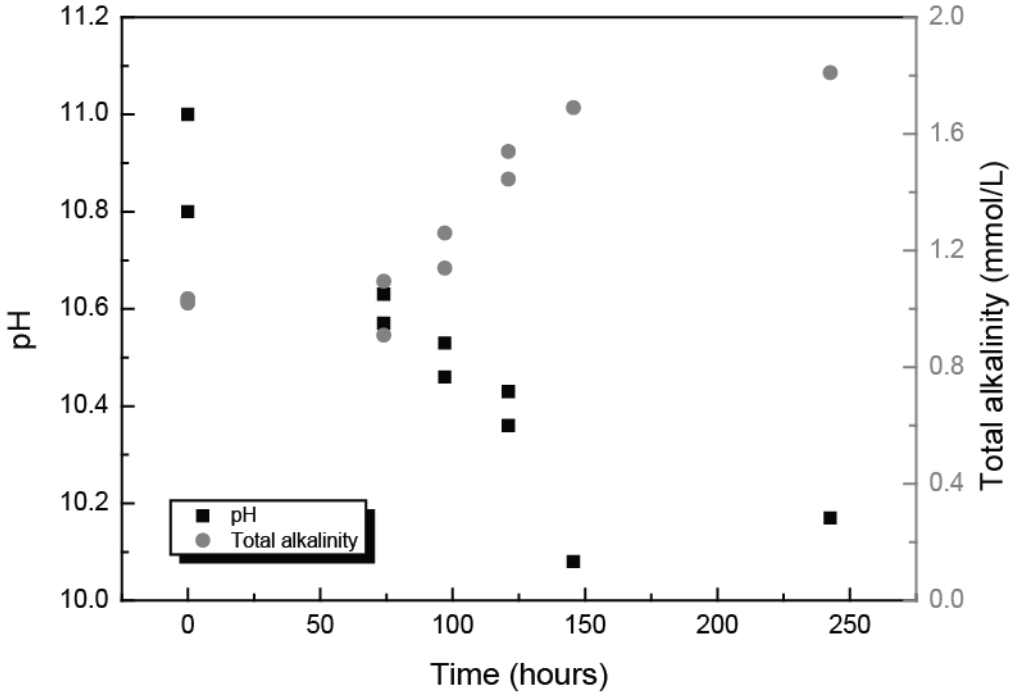
11.2
11.0
10.8
10.6
10.4
10.2
10.0
pH
2.0
1.6
1.2
0.8
0.4
0.0
Total alkalinity (mmol/L)
0
50
100
150
200
250
Time (hours)
pH
Total alkalinity

Figure 4

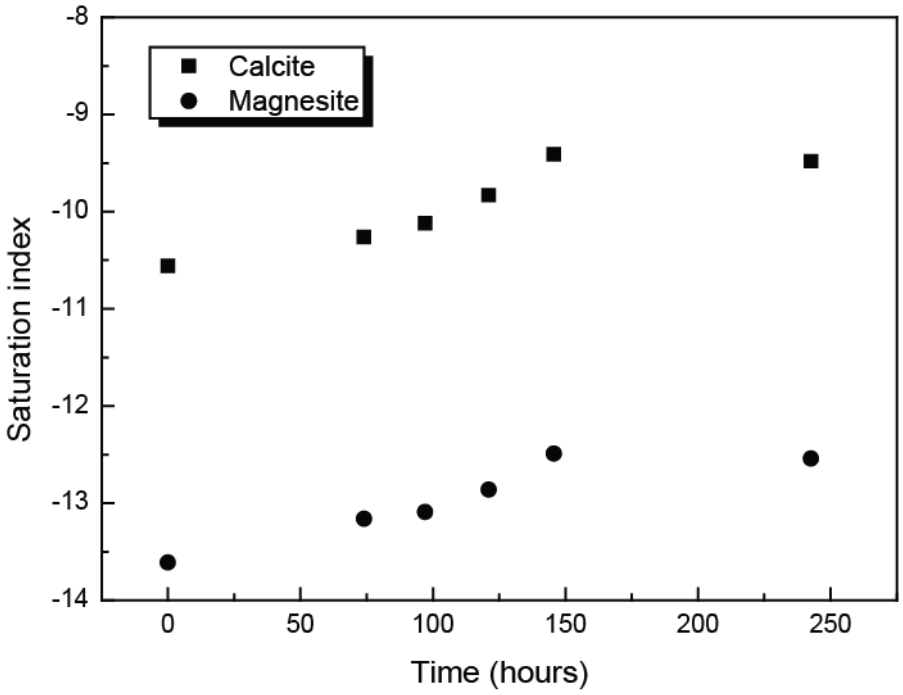
Calcite
Magnesite
Saturation index
Time (hours)
-8
-9
-10
-11
-12
-13
-14
0
50
100
150
200
250

Figure 5

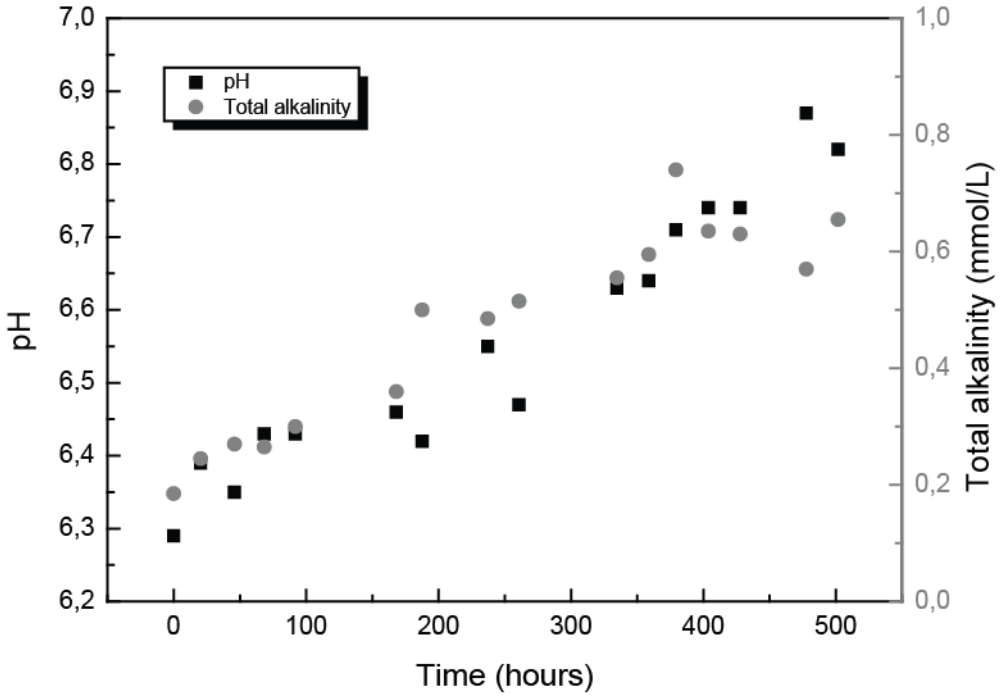
pH
Total alkalinity
pH
Total alkalinity (mmol/L)
Time (hours)
7,0
6,9
6,8
6,7
6,6
6,5
6,4
6,3
6,2
1,0
0,8
0,6
0,4
0,2
0,0
0
100
200
300
400
500

Figure 6

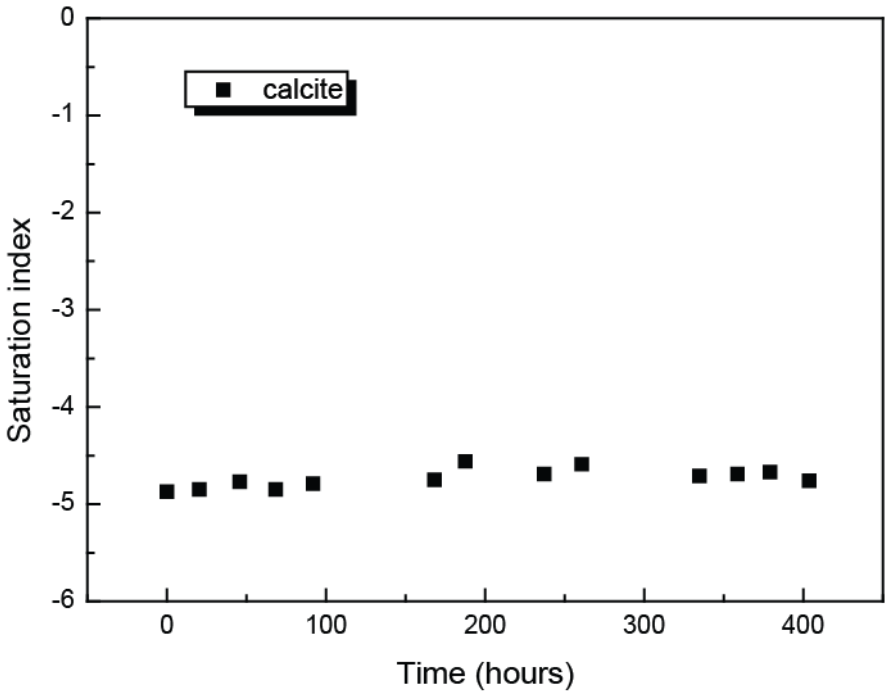
calcite
Saturation index
Time (hours)
0
-1
-2
-3
-4
-5
-6
0
100
200
300
400

Figure 7